

Inequivalence between the Euclidean and Lorentzian versions of the type IIB matrix model from Lefschetz thimble calculations

Chien-Yu CHOU,^{1,*} Jun NISHIMURA,^{1,2,†} and Ashutosh TRIPATHI^{1,‡}

¹*Graduate Institute for Advanced Studies, SOKENDAI, 1-1 Oho, Tsukuba, Ibaraki 305-0801, Japan*

²*KEK Theory Center, Institute of Particle and Nuclear Studies,*

High Energy Accelerator Research Organization, 1-1 Oho, Tsukuba, Ibaraki 305-0801, Japan

(Dated: January 30, 2025; preprint: KEK-TH-2686)

The type IIB matrix model is conjectured to describe superstring theory nonperturbatively in terms of ten $N \times N$ bosonic traceless Hermitian matrices A_μ ($\mu = 0, \dots, 9$), whose eigenvalues correspond to (9+1)-dimensional space-time. Quite often, this model has been investigated in its Euclidean version, which is well defined although the $SO(9, 1)$ Lorentz symmetry of the original model is replaced by the $SO(10)$ rotational symmetry. Recently, a well-defined model respecting the Lorentz symmetry has been proposed by “gauge-fixing” the Lorentz symmetry nonperturbatively using the Faddeev-Popov procedure. Here we investigate the two models by Monte Carlo simulations overcoming the severe sign problem by the Lefschetz thimble method, in the case of matrix size $N = 2$ omitting fermionic contributions. We add a quadratic term $\gamma \text{tr}(A_\mu A^\mu)$ in the action and calculate the expectation values of rotationally symmetric (or Lorentz symmetric) observables as a function of the coefficient γ . Our results exhibit striking differences between the two models around $\gamma = 0$ and in the $\gamma > 0$ region associated with the appearance of different saddle points, clearly demonstrating their inequivalence against naive expectations from quantum field theory.

Introduction— The type IIB matrix model [1] (or the Ishibashi-Kawai-Kitazawa-Tsuchiya model) has been attracting attention as a promising nonperturbative formulation of superstring theory analogous to the lattice gauge theory. In particular, not only space but also time is expected to emerge dynamically from the 10 bosonic $N \times N$ Hermitian matrices A_μ ($\mu = 0, \dots, 9$). From this viewpoint, the possibility of the emergence of (3 + 1)-dimensional space-time has been investigated intensively.

Historically, the emergence of 4D space-time was first discussed in the Euclidean model, which is well-defined [2, 3] although the $SO(9, 1)$ Lorentz symmetry of the original model is replaced by the $SO(10)$ rotational symmetry. The configurations that give the minimum action are diagonal up to $SU(N)$ symmetry, where the diagonal elements represent the 10D space-time coordinates. Based on the one-loop effective action around such configurations, it was argued that the fermionic zero modes may play a crucial role in collapsing the emergent space-time to lower dimensions [4].

The first nonperturbative calculation in the Euclidean model was carried out by the Gaussian expansion method, where it was shown that the $SO(10)$ symmetry is spontaneously broken down to $SO(3)$ [5]. This conclusion was confirmed also by numerical simulations [6], in which the phase of the Pfaffian that arises from integrating out fermionic matrices plays a crucial role [7, 8].

In the Lorentzian model, non-diagonal saddle-point configurations that describe expanding space-time were shown to appear if one adds a quadratic term (or the “mass term”) to the action [9–15], which is motivated as an infrared regularization [16]. Recent numerical studies [17–19] also suggest the emergence of expanding space-time, where only three out of nine spatial directions ex-

pand if fermionic contributions are included properly.

However, it was pointed out recently [20] that the partition function of a Lorentz symmetric model is *necessarily* divergent due to the noncompactness of the symmetry group, and it was proposed to remove this divergence by gauge-fixing the Lorentz symmetry using the Faddeev-Popov procedure. Thus a totally well-defined model respecting the Lorentz symmetry was obtained.

In this Letter, we perform Monte Carlo simulations of this “gauge-fixed” Lorentzian model for the first time in the case of matrix size $N = 2$ omitting fermionic contributions. Since the integrand of the partition function involves a phase factor, there is a severe sign problem. We overcome this problem by applying the Lefschetz thimble method (LTM) [21–26], which is based on firm mathematical grounds such as Cauchy’s theorem and the Picard-Lefschetz theory for deforming the integration contour in the complex plane. We obtain explicit results for Lorentz invariant observables as a function of the coefficient γ of the Lorentz invariant mass term.

We also perform simulations of the Euclidean model, which is obtained from the gauge-unfixed Lorentzian model by replacing $A_0 = -iA_{10}$. One might naively think that the two models are equivalent since they are related to each other by Wick rotation, which is commonly used in quantum field theory. However, our results exhibit striking differences between the two models, in particular, around $\gamma = 0$ and in the $\gamma > 0$ region associated with the appearance of different saddle points.

Saddles in the gauge-unfixed model— The partition function of the type IIB matrix model can be formally written as

$$Z = \int dA e^{iS_b[A]} \text{Pf} \mathcal{M}[A], \quad (1)$$

where A_μ ($\mu = 0, \dots, 9$) are $N \times N$ traceless Hermitian matrices. The bosonic action $S_b[A]$ is given by [1]

$$S_b[A] = -\frac{1}{4}N\text{tr}[A_\mu, A_\nu][A^\mu, A^\nu], \quad (2)$$

where the indices μ and ν are raised and lowered using the Lorentzian metric $\eta_{\mu\nu} = \text{diag}(-1, 1, \dots, 1)$ and repeated indices are summed over. The model has $\text{SO}(9, 1)$ Lorentz symmetry $A'_\mu = \mathcal{O}_{\mu\nu}A_\nu$, where $\mathcal{O} \in \text{SO}(9, 1)$, as well as the $\text{SU}(N)$ symmetry $A'_\mu = UA_\mu U^\dagger$, where $U \in \text{SU}(N)$. The Pfaffian $\text{Pf}\mathcal{M}[A] \in \mathbb{R}$ in (1) represents the contribution from the fermionic matrices, which makes the model maximally supersymmetric. In what follows, we omit the Pfaffian, and generalize the model to $D = d + 1$ dimensions, where d represents the number of spatial matrices.

The classical equation of motion or the saddle-point equation is given by

$$[A_\nu, [A^\nu, A_\mu]] = 0 \quad \text{for all } \mu = 0, 1, \dots, d. \quad (3)$$

One can easily prove that all the solutions are given by diagonal matrices up to the $\text{SU}(N)$ symmetry. (See Appendix A of Ref. [11], for instance.)

If one adds the Lorentz invariant mass term

$$S_m[A] = -\frac{1}{2}\gamma N \text{tr}(A_\mu A^\mu) \quad (4)$$

to the action, the saddle-point equation becomes

$$[A_\nu, [A^\nu, A_\mu]] = \gamma A_\mu \quad \text{for all } \mu = 0, 1, \dots, d. \quad (5)$$

The solutions of this equation for $\gamma \neq 0$ can be written in general as $A_\mu = \sqrt{|\gamma|}A_\mu^{(0)}$, where $A_\mu^{(0)}$ is some configuration independent of γ . Using the same rescaling, one also finds that the partition function (1) is dominated by some saddle-point configurations at large $|\gamma|$, where quantum corrections are suppressed by $1/\gamma^2$. Thus the “massless” limit $\gamma \rightarrow 0$ corresponds to the strong coupling limit.

Solutions of Eq. (5) were generated numerically [13] and they typically represent expanding space-time for $\gamma > 0$, where the number of expanding directions is left arbitrary at the classical level. For $\gamma < 0$, no such solutions were found.

Saddles in the gauge-fixed model— In Ref. [20], it was pointed out that the partition function (1) is actually divergent since all the Lorentz-boosted configurations contribute equally, and that a naive cutoff that breaks the Lorentz symmetry leaves a severe artifact even if one takes the limit of removing the cutoff eventually. However, this divergence is unphysical in the sense that it is simply due to the redundancy of description. Hence, a physically appropriate way to get rid of this divergence is to choose a representative of the configurations that are related to each other by Lorentz transformation and to integrate over the representative only. This can be done

by the Faddeev-Popov procedure, which is used also in fixing the gauge in gauge theories. The gauge-fixed model thus obtained [20] is given by

$$Z = \int dA \Delta_{\text{FP}}[A] \prod_{i=1}^d \delta(\text{tr}(A_0 A_i)) e^{i(S_b[A] + S_m[A])}, \quad (6)$$

where the δ -function represents the gauge-fixing condition $\text{tr}(A_0 A_i) = 0$ for $i = 1, \dots, d$. $\Delta_{\text{FP}}[A]$ represents the corresponding Faddeev-Popov (FP) determinant

$$\Delta_{\text{FP}}[A] = \det \Omega, \quad \Omega_{ij} = \text{tr}(A_0)^2 \delta_{ij} + \text{tr}(A_i A_j), \quad (7)$$

where Ω is a $d \times d$ real symmetric matrix.

The saddle-point equation in the gauge-fixed model (6) is given by

$$N[A_\nu, [A^\nu, A_\mu]] = \gamma N A_\mu + i \text{Tr} \left(\Omega^{-1} \frac{\partial \Omega}{\partial A^\mu} \right) \quad (8)$$

for all $\mu = 0, 1, \dots, d$. Since the gauge-fixed model (6) still has $\text{SO}(d)$ rotational symmetry, we use it to restrict ourselves to configurations with $\text{tr}(A_i A_j) = 0$ for $i \neq j$, which reduces the saddle-point equation (8) to

$$N[A_\nu, [A^\nu, A_\mu]] = (\gamma N + i\kappa_\mu) A_\mu \quad (\text{no sum over } \mu), \quad (9)$$

$$\kappa_i = 2 \{ \text{tr}(A_0)^2 + \text{tr}(A_i)^2 \}^{-1}, \quad \kappa_0 = \sum_{i=1}^d \kappa_i. \quad (10)$$

Thus we find that even for $\gamma = 0$, we obtain a mass-like term in (9) with the coefficients κ_μ determined by (10) in a self-consistent manner. This implies, in particular, that saddle points become non-diagonal even for $\gamma = 0$.

Moreover, due to the “ i ” on the right-hand side of (9), the saddle points become complex in general, which raises the issue of whether each saddle point is relevant in the sense of the Picard-Lefschetz theory. In this regard, we note that for large $|\gamma|$, the solutions of (9) reduce to the solutions of (5) for the gauge-unfixed model. Therefore, it is expected that the relevant saddle points at large $|\gamma|$ are given by complex solutions which are smoothly connected to real solutions of (5). By “real”, we actually mean *Hermitian* A_μ , which has *real* coefficients A_μ^α in the expansion $A_\mu = \sum A_\mu^\alpha t^\alpha$ in terms of the $\text{SU}(N)$ generators t^α . The word “complex” is used similarly.

The $N = 2$ case— To be concrete, let us consider the $N = 2$ case. In the gauge-unfixed Lorentzian model, the real solutions of (5) for $\gamma > 0$ are given by [27]

$$\begin{aligned} \text{(a)} \quad & A_\mu = 0, \\ \text{(b)} \quad & A_\mu = \sqrt{\frac{\gamma}{4}} \sigma_\mu \quad (\mu = 1, 2), \quad A_\mu = 0 \quad (\text{otherwise}), \\ \text{(c)} \quad & A_\mu = \sqrt{\frac{\gamma}{8}} \sigma_\mu \quad (\mu = 1, 2, 3), \quad A_\mu = 0 \quad (\text{otherwise}), \end{aligned} \quad (11)$$

where σ_i ($i = 1, 2, 3$) are the Pauli matrices. For $\gamma < 0$, the trivial one (a) is the only real solution.

In the gauge-fixed Lorentzian model, on the other hand, the general solution of the saddle-point equations can be parameterized as [28]

$$\begin{aligned} A_0 &= z \sigma_3, & A_1 &= x \sigma_1, & A_2 &= y \sigma_2, \\ A_i &= 0 \quad (i = 3, \dots, d), \end{aligned} \quad (12)$$

up to the $SU(2) \times SO(d)$ symmetry, where $x, y, z \in \mathbb{C}$. Here we have assumed $d \geq 4$ for simplicity. In this case, $A_0 \neq 0$ for finite γ since otherwise Ω^{-1} in (8) becomes singular. This fact plays an important role in the saddle-point structure in the gauge-fixed Lorentzian model.

Plugging (12) in (9) and (10) and solving them for x, y, z , we can obtain all the saddle points. In Fig. 1, we show the nine solutions for $\gamma = 30$ in the $\text{Re tr}(A_\mu A^\mu) - \text{Re tr}(A_0)^2$ plane. The solutions for $\gamma < 0$ can be obtained from those for $\gamma > 0$ with the same $|\gamma|$ by $A_\mu \mapsto iA_\mu$. For instance, the plot for $\gamma = -30$ can be obtained by rotating the one in Fig. 1 by 180 degrees.

These nine saddle points can be classified into the following four groups according to their asymptotic behaviors at large $|\gamma|$ up to symmetries.

$$\begin{aligned} \text{(I)} & A_\mu \sim 0, \\ \text{(II)} & A_\mu \sim \sqrt{\frac{\gamma}{4}} \sigma_\mu \quad (\mu = 1, 2), \quad A_\mu \sim 0 \quad (\text{otherwise}), \\ \text{(III)} & A_0 \sim i\sqrt{\frac{\gamma}{4}} \sigma_3, \quad A_1 \sim \sqrt{\frac{\gamma}{4}} \sigma_1, \quad A_\mu \sim 0 \quad (\text{otherwise}), \\ \text{(IV)} & A_0 \sim i\sqrt{\frac{\gamma}{8}} \sigma_3, \quad A_\mu \sim \sqrt{\frac{\gamma}{8}} \sigma_\mu \quad (\mu = 1, 2), \\ & A_\mu \sim 0 \quad (\text{otherwise}). \end{aligned} \quad (13)$$

For $\gamma > 0$, the solutions that become real at large γ are those in groups (I) and (II), which are smoothly connected to the solutions (a) and (b), respectively, in the gauge-unfixed model. There is no solution that is smoothly connected to (c) as anticipated from (12). For $\gamma < 0$, the solutions that become real at large $|\gamma|$ are those in group (I), which is smoothly connected to the solution (a) in the gauge-unfixed model. These solutions are the relevant saddle points at large $|\gamma|$. By changing γ continuously, we find that relevant saddles at $\gamma > 0$ are smoothly connected to irrelevant saddles at $\gamma < 0$ and vice versa, meaning that the group identification of each saddle can change as we cross $\gamma = 0$.

Defining the Euclidean model— So far, we have discussed the gauge-fixed Lorentzian model (6), which uses gauge fixing to remove the divergence of the original model due to the noncompact symmetry group.

An alternative way to render the partition function finite is to make a ‘‘Wick rotation’’ $A_0 = -iA_{10}$ with A_{10} being Hermitian. The Euclidean model obtained in this way is given by

$$Z_E = \int dA e^{i(S_b[A] + S_m[A])}, \quad (14)$$

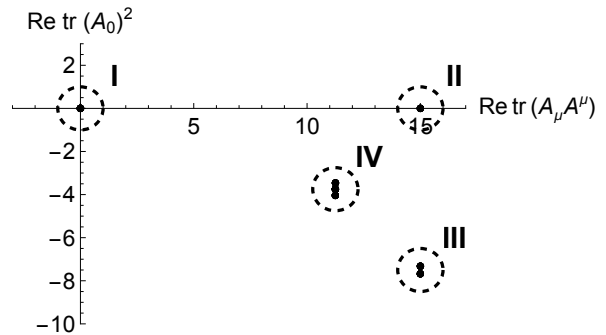


FIG. 1. The nine saddle points for $\gamma = 30$ are shown in the $\text{Re tr}(A_\mu A^\mu) - \text{Re tr}(A_0)^2$ plane. There are actually three distinct points near the origin, which are close to each other.

where the two terms $S_b[A]$ and $S_m[A]$ in the action are formally the same as (2) and (4), assuming that A represents A_μ ($\mu = 1, \dots, D$) and defining $A^D \equiv A_D$. Since the $SO(d, 1)$ Lorentz symmetry of the original model is converted into the $SO(D)$ rotational symmetry, there is no more divergence associated with the noncompactness of the symmetry group. In the $N = 2$ case, the saddle points are essentially the same as in the gauge-unfixed Lorentzian model given by (11) and below.

Note that the partition function of this Euclidean model still involves a phase factor in the integrand. The Euclidean model discussed in the literature involves e^{-S_b} instead, and it can be obtained by setting $\gamma = 0$ and making a contour deformation $A_\mu = e^{\frac{1}{8}\pi i} \tilde{A}_\mu$ ($\mu = 1, \dots, 10$) with \tilde{A}_μ being Hermitian. The model (14) may be viewed as a natural extension of this conventional Euclidean model to $\gamma \neq 0$, which may be compared directly with the gauge-fixed Lorentzian model with the same γ .

Monte Carlo simulations— Let us discuss our results based on the LTM for the gauge-fixed Lorentzian model and the Euclidean model in the $N = 2$ and $d = 4$ case.

Fig. 2 shows $\langle \text{tr}(A_\mu A^\mu) \rangle$ as a function of γ . First we discuss the results for the gauge-fixed Lorentzian model. At large $|\gamma|$, the results are expected to approach the results for some relevant saddle points discussed earlier. For $\gamma > 0$, the data points approach the red line representing the result for the saddle point in group (II) in (13). This saddle point continues to the one in group (IV) in the $\gamma < 0$ region, which is irrelevant. For $\gamma < 0$, the data points approach the blue line and the black line representing the results for the two saddle points in group (I) in (13). [The result for the third saddle point in group (I), which is not shown here, diverges at $\gamma = 0$.] The blue and black lines continue to the saddle points in groups (III) and (IV) in the $\gamma > 0$ region, respectively, which are irrelevant there. Thus we observe a switching of the (dominant) relevant saddle points as we cross $\gamma = 0$. At $\gamma \sim 0$, we observe some oscillating behavior, which may be due to interference between different saddles.

Let us turn our attention to the results for the Eu-

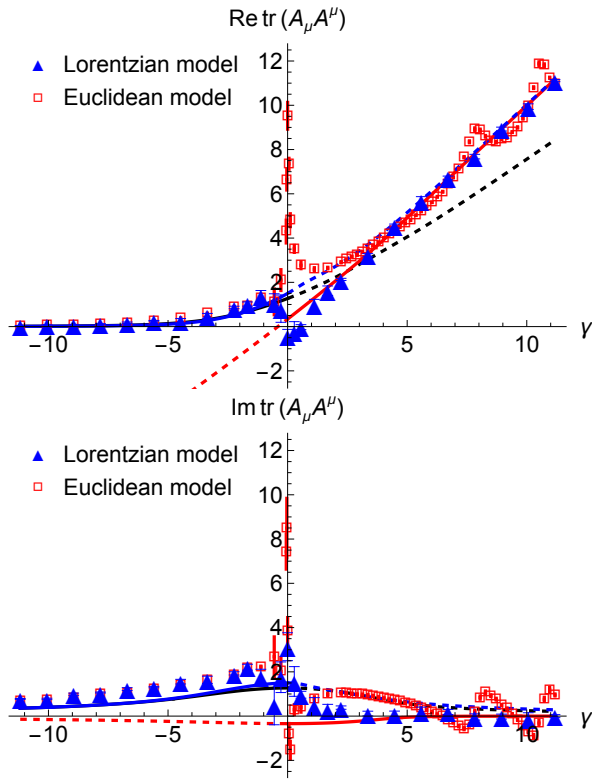


FIG. 2. The real part (Top) and the imaginary part (Bottom) of $\langle \text{tr}(A_\mu A^\mu) \rangle$ are plotted against γ for the gauge-fixed Lorentzian model (blue triangles) and the Euclidean model (red squares). The red line represents the result obtained for the relevant saddle in group (II) at $\gamma > 0$, while the black line and the blue line represent the results obtained for the relevant saddles in group (I) at $\gamma < 0$. Each of them continue to irrelevant saddles as one crosses $\gamma = 0$, which are indicated by the dashed line with the same color.

clidean model. In the $\gamma > 0$ region, we see a clear oscillating behavior, which is due to the interference between the two dominant saddle points (b) and (c) in (11). The partition functions Z_b and Z_c around these two saddles can be calculated perturbatively [27], and their ratio is given by $Z_b/Z_c \sim 2e^{-i\gamma^2/8}$ at large γ . We can therefore make an estimate

$$\langle \text{tr}(A_\mu A^\mu) \rangle \sim \frac{\langle \text{tr}(A_\mu A^\mu) \rangle_b Z_b + \langle \text{tr}(A_\mu A^\mu) \rangle_c Z_c}{Z_b + Z_c}, \quad (15)$$

with $\langle \text{tr}(A_\mu A^\mu) \rangle_b \sim \gamma$ and $\langle \text{tr}(A_\mu A^\mu) \rangle_c \sim \frac{3}{4}\gamma$, which roughly explains the oscillating behavior.

In the $\gamma < 0$ region, the data points for the two models get close to each other as $|\gamma|$ increases. This is understandable since the dominant saddle points are essentially the trivial one $A_\mu = 0$ in the $\gamma \rightarrow -\infty$ limit for both models. In fact, the asymptotic behavior of the partition functions (6) and (14) is readily obtained by just omitting the quartic term S_b and rescaling $A_\mu \mapsto A_\mu/\sqrt{|\gamma|}$, which yields the common result $Z \sim |\gamma|^{-3D/2}$. One can then obtain $\langle \text{tr}(A_\mu A^\mu) \rangle = i\frac{2}{N} \frac{d}{d\gamma} \log Z = \frac{3Di}{N|\gamma|}$. In Fig. 3, we

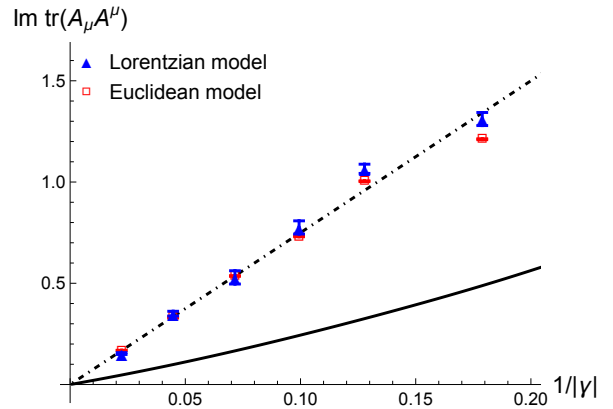


FIG. 3. The imaginary part of $\langle \text{tr}(A_\mu A^\mu) \rangle$ is plotted against $1/|\gamma|$ for the gauge-fixed Lorentzian model (blue triangles) and the Euclidean model (red squares). The dot-dashed line represents the leading behavior $\frac{15/2}{|\gamma|}$ obtained by omitting the quartic term S_b . The solid line represents the leading behavior $\frac{4}{|\gamma|}$ obtained from the saddle points in group (I).

plot the imaginary part of $\langle \text{tr}(A_\mu A^\mu) \rangle$ against $1/|\gamma|$ for the two models, which agrees with the predicted asymptotic behavior. On the other hand, we also see clear discrepancies showing up already at $|\gamma| \lesssim 10$, which suggest that the agreement holds only in the leading behavior.

Incidentally, let us note that the asymptotic behavior obtained here cannot be reproduced by the relevant saddle points in the gauge-fixed Lorentzian model in the $\gamma < 0$ region. This is due to the fact that the Faddeev-Popov determinant $\Delta_{\text{FP}}[A]$ in (6) becomes zero for the saddle points in group (I) at $\gamma \rightarrow -\infty$.

Finally let us comment on the prominent peak observed in Fig. 2 around $\gamma = 0$ for the Euclidean model. This is actually due to the emergence of commuting saddles represented by diagonal solutions to (3) at $\gamma = 0$, which do not occur in the gauge-fixed Lorentzian model. This can be confirmed by calculating a quantity

$$\rho = \left| \frac{\langle -\text{tr}([A_\mu, A_\nu][A^\mu, A^\nu]) \rangle}{\langle \text{tr}(A_\mu A^\mu) \rangle^2} \right| \quad (16)$$

that probes the noncommutativity of the dominant configurations, which shows a sharp dip around $\gamma = 0$ as a function of γ in the Euclidean model [29].

Discussions— In this Letter, we have investigated the impact of the Wick rotation on the nonperturbative dynamics of the type IIB matrix model. In particular, this problem has become clearer than ever, now that we have two well-defined models, namely the Euclidean model with the $\text{SO}(D)$ rotational symmetry on one hand and the Lorentzian model with the $\text{SO}(d, 1)$ Lorentz symmetry on the other hand, which are related to each other by the Wick rotation. In defining the latter model, the Lorentz symmetry has to be gauge-fixed properly by the Faddeev-Popov procedure in order to remove the appar-

ent divergence due to the noncompact symmetry group.

In quantum field theory, the Euclidean theory obtained by the Wick rotation is often used to investigate the properties of the vacuum and the excitations around it through the calculations of vacuum expectation values and correlation functions. The Euclidean theory is also used in investigating quantum tunneling semi-classically through instantons, and such calculations are extended even to quantum gravity. The Euclidean theory also forms the basis of the lattice gauge theory, which plays an important role in defining gauge theories nonperturbatively. For these reasons, we tend to consider that the Euclidean theory and the Lorentzian theory are equivalent. This point of view has been taken in the type IIB matrix model, and the Euclidean version has been studied intensively in the literature.

In order to give a clear answer to this equivalence issue, we have investigated the Euclidean and Lorentzian models adding a mass term, which seems to play an important role in the emergence of space-time. In the simplest $N = 2$ case omitting the fermionic contributions, we have obtained nonperturbative results as a function of γ by Monte Carlo simulations overcoming the severe sign problem by the LTM. While the two models show the same asymptotic behavior for $\gamma \rightarrow -\infty$ due to the dominance of the trivial saddle A_μ there, otherwise they give totally different behaviors in the whole region of γ . In particular, in the $\gamma > 0$ region, the saddle points (b) and (c) in (11) dominate in the Euclidean model, whereas only the saddle point (b) dominates in the Lorentzian model. At $\gamma \sim 0$, the commuting saddles appear in the Euclidean model, whereas they do not show up in the Lorentzian model. Thus our results clearly demonstrate that the two models are inequivalent.

We are currently trying to extend our numerical simulations to larger N and to the supersymmetric case. Recently the Euclidean model with supersymmetric mass deformation [30] has been attracting attention since its gravity dual has been identified [31–33]. This gives a new perspective to the emergence of space-time in the type IIB matrix model. It would be also interesting to investigate this model and its Lorentzian version by numerical simulations. Another important direction is to identify the gravity dual of the Lorentzian models.

Acknowledgments— We thank Yuhma Asano, Worapat Piensuk and Naoyuki Yamamori for valuable discussions on the related project [27], and Cheng-Tsung Wang for his proof [28] for the form (12) of general solutions. This work was supported by JST, the establishment of university fellowships towards the creation of science technology innovation, Grant Number JPMJFS2136.

[†] jnishi@post.kek.jp

[‡] tripashu@post.kek.jp

- [1] N. Ishibashi, H. Kawai, Y. Kitazawa, and A. Tsuchiya, A Large N reduced model as superstring, Nucl. Phys. B **498**, 467 (1997), arXiv:hep-th/9612115.
- [2] W. Krauth, H. Nicolai, and M. Staudacher, Monte Carlo approach to M theory, Phys. Lett. B **431**, 31 (1998), arXiv:hep-th/9803117.
- [3] P. Austing and J. F. Wheeler, Convergent Yang-Mills matrix theories, JHEP **04**, 019, arXiv:hep-th/0103159.
- [4] H. Aoki, S. Iso, H. Kawai, Y. Kitazawa, and T. Tada, Space-time structures from IIB matrix model, Prog. Theor. Phys. **99**, 713 (1998), arXiv:hep-th/9802085.
- [5] J. Nishimura, T. Okubo, and F. Sugino, Systematic study of the SO(10) symmetry breaking vacua in the matrix model for type IIB superstrings, JHEP **10**, 135, arXiv:1108.1293 [hep-th].
- [6] K. N. Anagnostopoulos, T. Azuma, Y. Ito, J. Nishimura, T. Okubo, and S. Kovalev Papadoudis, Complex Langevin analysis of the spontaneous breaking of 10D rotational symmetry in the Euclidean IKKT matrix model, JHEP **06**, 069, arXiv:2002.07410 [hep-th].
- [7] J. Nishimura and G. Vernizzi, Spontaneous breakdown of Lorentz invariance in IIB matrix model, JHEP **04**, 015, arXiv:hep-th/0003223.
- [8] J. Nishimura and G. Vernizzi, Brane world from IIB matrices, Phys. Rev. Lett. **85**, 4664 (2000), arXiv:hep-th/0007022.
- [9] S.-W. Kim, J. Nishimura, and A. Tsuchiya, Expanding universe as a classical solution in the Lorentzian matrix model for nonperturbative superstring theory, Phys. Rev. D **86**, 027901 (2012), arXiv:1110.4803 [hep-th].
- [10] S.-W. Kim, J. Nishimura, and A. Tsuchiya, Late time behaviors of the expanding universe in the IIB matrix model, JHEP **10**, 147, arXiv:1208.0711 [hep-th].
- [11] H. C. Steinacker, Cosmological space-times with resolved Big Bang in Yang-Mills matrix models, JHEP **02**, 033, arXiv:1709.10480 [hep-th].
- [12] H. C. Steinacker, Quantized open FRW cosmology from Yang-Mills matrix models, Phys. Lett. **B782**, 176 (2018), arXiv:1710.11495 [hep-th].
- [13] K. Hatakeyama, A. Matsumoto, J. Nishimura, A. Tsuchiya, and A. Yosprakob, The emergence of expanding space-time and intersecting D-branes from classical solutions in the Lorentzian type IIB matrix model, PTEP **2020**, 043B10 (2020), arXiv:1911.08132 [hep-th].
- [14] M. Sperling and H. C. Steinacker, Covariant cosmological quantum space-time, higher-spin and gravity in the IKKT matrix model, JHEP **07**, 010, arXiv:1901.03522 [hep-th].
- [15] H. C. Steinacker, Gravity as a quantum effect on quantum space-time, Phys. Lett. B **827**, 136946 (2022), arXiv:2110.03936 [hep-th].
- [16] S.-W. Kim, J. Nishimura, and A. Tsuchiya, Expanding (3+1)-dimensional universe from a Lorentzian matrix model for superstring theory in (9+1)-dimensions, Phys. Rev. Lett. **108**, 011601 (2012), arXiv:1108.1540 [hep-th].
- [17] K. Hatakeyama, K. Anagnostopoulos, T. Azuma, M. Hirasawa, Y. Ito, J. Nishimura, S. Papadoudis, and A. Tsuchiya, Complex Langevin studies of the emergent space-time in the type IIB matrix model (2022) arXiv:2201.13200 [hep-th].
- [18] J. Nishimura, Signature change of the emergent space-

* ccy@post.kek.jp

- time in the IKKT matrix model, PoS **CORFU2021**, 255 (2022), arXiv:2205.04726 [hep-th].
- [19] K. N. Anagnostopoulos, T. Azuma, K. Hatakeyama, M. Hirasawa, Y. Ito, J. Nishimura, S. K. Papadoudis, and A. Tsuchiya, Progress in the numerical studies of the type IIB matrix model, Eur. Phys. J. ST **232**, 3681 (2023), arXiv:2210.17537 [hep-th].
- [20] Y. Asano, J. Nishimura, W. Piensuk, and N. Yamamori, Defining the type iib matrix model without breaking lorentz symmetry (2025), arXiv:2404.14045 [hep-th].
- [21] E. Witten, Analytic continuation of chern-simons theory (2010), arXiv:1001.2933 [hep-th].
- [22] M. Cristoforetti, F. Di Renzo, and L. Scorzato, New approach to the sign problem in quantum field theories: High density qcd on a lefschetz thimble, Physical Review D **86**, 10.1103/physrevd.86.074506 (2012).
- [23] M. Cristoforetti, F. Di Renzo, A. Mukherjee, and L. Scorzato, Monte carlo simulations on the lefschetz thimble: Taming the sign problem, Physical Review D **88**, 10.1103/physrevd.88.051501 (2013).
- [24] H. Fujii, D. Honda, M. Kato, Y. Kikukawa, S. Komatsu, and T. Sano, Hybrid monte carlo on lefschetz thimbles — a study of the residual sign problem, Journal of High Energy Physics **2013**, 10.1007/jhep10(2013)147 (2013).
- [25] A. Alexandru, G. Basar, P. F. Bedaque, G. W. Ridgway, and N. C. Warrington, Sign problem and monte carlo calculations beyond lefschetz thimbles (2016), arXiv:1512.08764 [hep-lat].
- [26] M. Fukuma, N. Matsumoto, and N. Umeda, Implementation of the hmc algorithm on the tempered lefschetz thimble method (2020), arXiv:1912.13303 [hep-lat].
- [27] Y. Asano, J. Nishimura, W. Piensuk, and N. Yamamori, in preparation.
- [28] C.-T. Wang, private discussion.
- [29] C.-Y. Chou, J. Nishimura, and A. Tripathi, in preparation.
- [30] G. Bonelli, Matrix strings in pp wave backgrounds from deformed superYang-Mills theory, JHEP **08**, 022, arXiv:hep-th/0205213.
- [31] S. A. Hartnoll and J. Liu, The polarised ikkt matrix model (2024), arXiv:2409.18706 [hep-th].
- [32] S. Komatsu, A. Martina, J. Penedones, A. Vuignier, and X. Zhao, Einstein gravity from a matrix integral – part i (2024), arXiv:2410.18173 [hep-th].
- [33] S. Komatsu, A. Martina, J. Penedones, A. Vuignier, and X. Zhao, Einstein gravity from a matrix integral – part ii (2024), arXiv:2411.18678 [hep-th].